

# Discovery and Validation of Circulating Hsa-miR-210-3p as a Potential Biomarker for Primary Open-Angle Glaucoma

Yaoming Liu, Yayi Wang, Yang Chen, Xiuli Fang, Tao Wen, Mianli Xiao, Shida Chen, and Xiulan Zhang

Zhongshan Ophthalmic Center, State Key Laboratory of Ophthalmology, Sun Yat-sen University, Guangzhou, People's Republic of China

Correspondence: Xiulan Zhang, Zhongshan Ophthalmic Center, State Key Laboratory of Ophthalmology, Sun Yat-sen University, 7S Jinsui Road, Guangzhou 510623, China; zhangxl2@mail.sysu.edu.cn.

Shida Chen, Zhongshan Ophthalmic Center, State Key Laboratory of Ophthalmology, Sun Yat-sen University, 7S Jinsui Road, Guangzhou 510623, China; chenshd3@mail.sysu.edu.cn.

YL and YW contributed equally to the work presented here and should therefore be regarded as equivalent authors.

Submitted: January 16, 2019

Accepted: June 4, 2019

Citation: Liu Y, Wang Y, Chen Y, et al. Discovery and validation of circulating hsa-miR-210-3p as a potential biomarker for primary open-angle glaucoma. *Invest Ophthalmol Vis Sci*. 2019;60:2925-2934. <https://doi.org/10.1167/iovs.19-26663>

**PURPOSE.** Blood-based examination tools for glaucoma diagnosis in clinical practice, which can be useful for screening patients when traditional ophthalmic examinations cannot be utilized, are not available thus far. This study aimed to identify circulating microRNAs (miRNAs) associated with primary open-angle glaucoma (POAG) and explore their utility as diagnostic markers.

**METHODS.** A total of 136 POAG patients and controls were enrolled. Next-generation RNA sequencing was used to explore the expression profile of circulating miRNAs in the sequencing set, and potential miRNAs from independent samples in both the screening and validation sets were validated by quantitative real-time polymerase chain reaction (qRT-PCR). Receiver operating characteristic (ROC) analysis was used to evaluate the ability of certain miRNAs to distinguish POAG patients from control subjects.

**RESULTS.** Using sequencing and qRT-PCR, hsa-miR-210-3p was found to be elevated in POAG patients in all sets. ROC analysis of the screening and validation sets revealed that hsa-miR-210-3p differentiated between POAG patients and matched controls with an area under the curve (AUC) of 0.846 (sensitivity: 84.6%; specificity: 80.8%) and 0.813 (sensitivity: 84.8%; specificity: 69.7%), respectively. In case of all nonsequencing participants, analysis revealed that hsa-miR-210-3p differentiated between severe POAG patients and controls with an AUC of 0.880 (sensitivity: 85.4%; specificity: 85.7%). In addition, the expression of hsa-miR-210-3p was associated with visual field defects of  $|\text{mean deviation}|$  ( $\beta = 0.237$ ;  $P = 0.022$ ) and average retinal nerve fiber layer thickness ( $\beta = -5.792$ ;  $P = 0.014$ ).

**CONCLUSIONS.** Circulating hsa-miR-210-3p may serve as a potential diagnostic marker for POAG (especially for severe POAG patients).

**Keywords:** POAG, biomarker, circulating microRNA, next-generation sequencing

Glaucoma, an ocular neurodegenerative disease, is the leading cause of irreversible blindness worldwide.<sup>1</sup> Primary open-angle glaucoma (POAG) is the most common subtype of glaucoma; the global number of POAG patients (people aged 40–80 years) was estimated to be 44.11 million in 2013, increasing to 52.68 million in 2020 and 79.76 million in 2040.<sup>2</sup> Unfortunately, the early diagnosis of POAG with irreversible optic neuropathy remains unsatisfactory thus far, which aggravates the global burden of glaucoma. Furthermore, blood-based examination tools for POAG diagnosis in clinical practice, which can be useful for screening patients when other ophthalmic examinations cannot be utilized, are not available thus far. To evaluate biomarkers by the collection of blood samples is safe and minimally invasive; therefore, developing a blood-based biomarker of POAG is promising and of great significance in clinical practice.

MicroRNAs (miRNAs) are small noncoding RNA molecules containing 19 to 22 nucleotides; they function in the posttranscriptional regulation of gene expression.<sup>3</sup> They are stable and often specifically enriched in a particular tissue or during essential cellular processes.<sup>4</sup> An increasing number of extracellular miRNAs from biofluids are being identified as biomarkers for cardiovascular disease, cancer, diabetes, ocular

disease, and many other disorders.<sup>5–12</sup> In our previous study, we identified glaucoma-specific miRNAs in the aqueous humor by next-generation sequencing.<sup>13</sup> However, collecting aqueous humor from patients was associated with high risk and could not be performed commonly.

In this study, we used next-generation sequencing to analyze individual serum samples from POAG patients and matched controls to identify specific miRNA expression characteristics in POAG patients and evaluate the potential of these miRNAs to serve as biomarkers for the diagnosis and grading of POAG.

## SUBJECTS AND METHODS

### Subjects

This research was conducted in accordance with the Declaration of Helsinki and with the approval of the Zhongshan Ophthalmic Center Institutional Review Board. Written informed consent was obtained from the patients and matched subjects at the Zhongshan Ophthalmic Center, Guangzhou, China. The POAG patients were enrolled from the outpatient glaucoma department, and participants without any evidence of POAG in either eye (control group) were also enrolled.



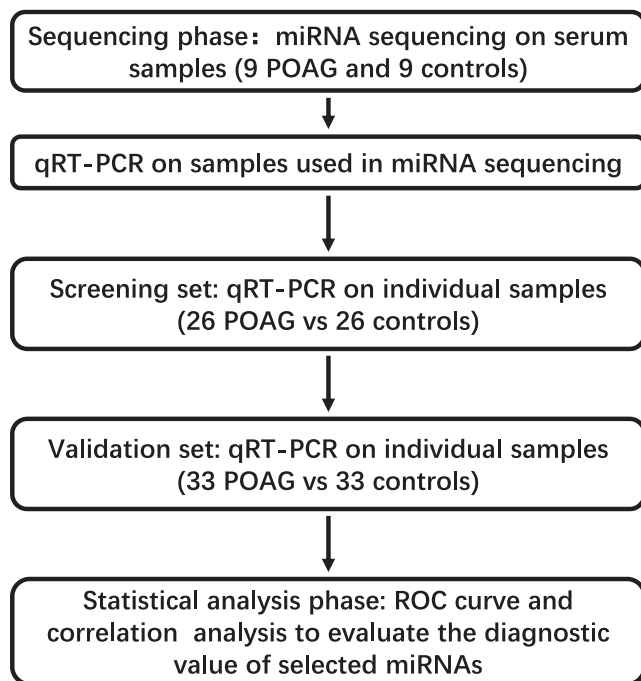


FIGURE 1. An overview of the experimental design.

The POAG diagnosis criteria were the same as those in our previous study<sup>14</sup>: (1) history of intraocular pressure (IOP) higher than 21 mm Hg, (2) open angles on gonioscopy, (3) glaucomatous optic disc damage (vertical cup-to-disc ratio >0.7, and/or interocular asymmetry of cup-to-disc ratio >0.2, and/or focal rim notching), with (4) corresponding visual field defect, and (5) exclusion of secondary causes.

All POAG patients underwent serial ophthalmic examinations, which were conducted by an experienced glaucoma specialist. The visual field was detected by the Humphrey computerized automated perimeter (Humphrey Field Analyzer; Carl Zeiss Meditec, Dublin, CA, USA). The condition of the eye was defined as mild when the mean deviation (MD) was  $\geq -6$  dB and as severe when the MD was  $< -6$  dB. The patient was defined as a mild POAG patient when the MD was  $\geq -6$  dB in both eyes and as a severe POAG patient when the MD was  $< -6$  dB in at least one eye. In addition, the retinal nerve fiber layer thickness (RNFLT) of the eyes of POAG patients was detected by deep range imaging optical coherence tomography (Atlantis, DRI OCT-1; Topcon, Tokyo, Japan). Medication use in POAG patients was recorded. The control subjects enrolled in this study underwent IOP measurement and fundus examination by an experienced glaucoma specialist to exclude the diagnosis of glaucoma. Participants (both POAG patients and controls) were excluded if they were found to suffer from ocular diseases other than age-related cataract. Participants with diabetes, hypertension, hyperthyroidism, immune-related diseases, and cancer were also excluded. A multiphase, cross-sectional observational study design was used to identify serum miRNAs as surrogate markers for POAG (Fig. 1).

### Serum Samples

Venous blood samples (3–5 mL) were collected from all patients and controls. Serum separation was accomplished by centrifugation at 1500g for 10 minutes, followed by a 10-minute high-speed centrifugation at 12,000g to completely remove the cell debris. The supernatant serum was recovered and stored at  $-80^{\circ}\text{C}$  until analysis.

### Library Preparation and Sequencing

Synthetic *Caenorhabditis elegans* miR-39 spike-in control was added to the serum, and RNA was extracted using a reagent (TRIzol LS Reagent; Life Technologies Corp., Carlsbad, CA, USA), according to the manufacturer's instructions. The library preparation and sequencing processes were the same as those in our previous study.<sup>13</sup> All extracted RNA from each serum sample was used to generate sequencing libraries. RNA segments of different sizes were separated by PAGE. An 18 to 30-nucleotide (nt) strip was recycled and ligated, with specific adapters, to the 3' and 5' ends. Adapter-ligated libraries were reverse-transcribed and amplified by PCR with primers containing index sequences specific for each sample. The purified PCR constructs were recovered by PAGE. The recycled products were dissolved in ethidium bromide solution and labeled. The quality and production of the prepared library were tested. Individual libraries were pooled and sequenced on a platform (HiSeq4000 platform; Illumina, Inc., San Diego, CA, USA).

### Sequencing Data Analysis

After obtaining raw data, we conducted a bioinformatics analysis according to previous studies.<sup>15–20</sup> The 49-nt sequence tags from the next-generation sequencing were subjected to a data cleaning analysis, which included getting rid of the low-quality tags, or the 5' adaptor contaminants from the 50-nt tags, to obtain clean, credible tags. Samples with adequate data output (clean tag count > 20,000,000) were used for further data analyses. Anchor alignment-based small RNA annotation was used to map clean reads to the reference genome and miRNA database (mirBase, available in the public domain, <http://www.mirbase.org/>). The miRNA expression level was calculated by using the TPM (transcripts per kilobase million) value. Only miRNAs annotated as mature in the mirBase data (mirbase21.0) were included. Differentially expressed miRNAs between two groups were screened by the NOISeq method. First, NOISeq built a noise distribution model according to the  $\log_2$  (fold change) value M and the absolute different value D of all pair conditions by using the sample's miRNA expression data in each group. Second, for miRNA-X, NOISeq computed its average expression "Control\_avg" in the control group and "Treat\_avg" in the treatment group. Then, the fold change M ( $M_X = \log_2[(\text{Treat\_avg})/(\text{Control\_avg})]$ ) and absolute different value D ( $D_X = |\text{Control\_avg} - \text{Treat\_avg}|$ ) were recorded. If M<sub>X</sub> and D<sub>X</sub> markedly diverged from the noise distribution model, miRNA-X was defined as a differentially expressed miRNA. We also used a probability value to assess how M<sub>X</sub> and D<sub>X</sub> both diverge from the noise distribution model. Finally, we screened differentially expressed small RNAs according to the following default criteria: fold change  $\geq 4$  and divergence probability  $\geq 0.8$ .

### Quantitative PCR (qPCR)

As described in our previous study,<sup>13</sup> serum samples were similarly cleared of potential debris by centrifugation. A *C. elegans* miR-39 spike-in control<sup>21</sup> was added to 100  $\mu\text{L}$  of the supernatant, and small RNAs were extracted using an extraction kit (miRNeasy SerumPlasma Kit; Qiagen, Hilden, Germany) in accordance with the manufacturer's instructions. RNA quality was evaluated using the Nanodrop system (ThermoScientific, Waltham, MA, USA). RNA samples with a concentration >4.0 ng/ $\mu\text{L}$  and those in which the total RNA amount was >50 ng were included for further analysis. Retrotranscription primers (stem loop) and qPCR primers (forward and reverse) for each miRNA were designed by

TABLE 1. Baseline Demographics and Participant Characteristics

Characteristics	Sequencing Set		Screening Set		Validation Set	
	POAG	NCs	POAG	NCs	POAG	NCs
Total, <i>n</i>	9	9	26	26	33	33
Age, mean (SD), y	60.4 (7.8)	62.8 (8.7)	39.8 (12.1)	39.6 (13.7)	41.2 (12.7)	42.8 (11.1)
Male, <i>n</i> (%)	9 (100)	9 (100)	20 (77.0)	18 (69.2)	25 (75.8)	26 (78.8)
IOP, mean (SD), mm Hg*†	22.9 (7.9)	13.2 (2.8)	15.9 (3.1)	13.6 (2.5)	17.4 (4.7)	14.1 (3.7)
Number of drugs, mean (SD), <i>n</i> †	1.8 (0.8)	0 (0)	1.5 (0.9)	0 (0)	1.3 (0.9)	0 (0)
MD, mean (SD), dB†	-15.3 (12.1)	N/A	-13.4 (9.0)	N/A	-12.3 (8.5)	N/A
RNFLTa, mean (SD), $\mu\text{m}\dagger$	58.3 (18.6)	N/A	63.6 (17.2)	N/A	69.0 (16.4)	N/A

N/A, data not available.

\* For the last visits before blood sampling.

† For the more severe eye.

RiboBio (Guangzhou, China). Subsequently, a commercial kit (miDETECT A Track miRNA qRT-PCR Starter Kit; RiboBio, Guangzhou, China) was used for reverse transcription and the qPCR-based detection of the selected miRNAs, in accordance with the manufacturer's instructions. The  $2^{-\Delta\Delta\text{CT}}$  method<sup>22</sup> was used as a relative quantification strategy for quantitative real-time (qRT)-PCR data in our study. We set a mean value of  $\Delta\text{CT}$  in all control samples ( $\text{avg}_{\Delta\text{CTcontrol}}$ ) as a standard, then  $\Delta\text{CT}$  of all samples from control and POAG groups were deducted by  $\text{avg}_{\Delta\text{CTcontrol}}$  to get individual  $\Delta\Delta\text{CT}$ . After using  $2^{-\Delta\Delta\text{CT}}$  to calculate fold changes, final fold changes of controls were not exactly "1 fold" but around "1 fold."

### General Statistical Analysis

Statistical analyses were performed using statistical software (SPSS Statistics 19.0; IBM Corp., Armonk, NY, USA). Data for continuous variables were presented as the means and standard errors (mean  $\pm$  SEM). For comparison between two groups, the Mann-Whitney *U* test or Student's *t*-test were used, as appropriate. Outliers were identified when values were greater than the mean  $\pm$  3\*SD. For categorical variables, we used the Fisher's exact test or the  $\chi^2$  test. All tests performed were two-sided, and  $P < 0.05$  were considered statistically significant. Receiver operating characteristic (ROC) analysis was utilized to assess the ability of miRNA expression to distinguish POAG patients from the controls. The cutoff value with the highest Youden index was selected within the test set and verified in the validation set, and the corresponding sensitivity and specificity were calculated. We also examined the capacity of miRNA expression to distinguish mild and severe glaucoma using ROC analysis. Linear regressions were used to characterize the relationship of the miRNA levels with the IOP, MD, and RNFLT average (RNFLTa) of the more severe eye (the eye with more severe visual field defects), the milder eye (the eye with milder visual field defects), and the average of both eyes, separately. Two models were fit: a simple model and a model adjusted for age, sex, and glaucoma medication.

## RESULTS

### Basic Clinical Characteristics of the Subjects

The patients and control subjects included in each phase were matched with respect to age. Nine POAG patients and nine matched controls were selected for sequencing. For the screening phase, we included 26 POAG patients and 26 matched controls. Furthermore, 33 independent POAG patients and 33 matched controls were enrolled for the validation phase. A total of 68 patients were enrolled (37 patients with bilateral POAG and 31 patients with unilateral POAG). There

was no significant clinical difference between the screening and validation sets, except for the enrolling time. Participants in the screening set were enrolled before those in the validation set. The basic clinical characteristics of the subjects are summarized in Table 1.

### Characteristics of Next-Generation Sequencing and miRNA Expression

Of the genome-wide miRNAs that were examined by miRNA sequencing, a total of 525 miRNAs were detected in the serum of control subjects and 522 miRNAs were detected in the serum of patients with POAG (Supplemental Excel S1). We screened differentially expressed miRNAs according to the following default criteria: fold change  $\geq 4$  and divergence probability  $\geq 0.8$ . Based on these criteria, hsa-miR-210-3p, hsa-miR-885-5p, and hsa-miR-3149 were identified as differentially expressed miRNAs in the POAG group (Table 2; Fig. 2). In addition, we performed qRT-PCR to verify the expression of hsa-miR-885-5p, hsa-miR-210-3p, and hsa-miR-3149 in the sequenced samples; the results were consistent with those of sequencing (Hsa-miR-885-5p: control:  $1.33 \pm 0.18$  fold,  $n = 9$ ; POAG:  $7.68 \pm 2.03$  fold,  $n = 9$ ;  $P = 0.003$  and Hsa-miR-210-3p: control:  $1.00 \pm 0.33$  fold,  $n = 9$ ; POAG:  $3.85 \pm 1.10$  fold,  $n = 9$ ;  $P = 0.016$ ) (Fig. 3). However, we failed to detect miRNA-3149, which was detected in the sequencing data (melting curves of hsa-miR-3149 in qRT-PCR were below standard). This might result from differences in reproducibility among various platforms such as small RNA sequencing, qRT-qPCR, and microarrays.<sup>23</sup>

### miRNA Levels in the Screening and Validation Sets

Next, we examined hsa-miR-885-5p and hsa-miR-210-3p in an independent screening sample using qRT-PCR (Fig. 4). In the independent screening set, hsa-miR-210-3p was consistently upregulated in the serum of POAG patients (Hsa-miR-210-3p: control:  $1.05 \pm 0.08$  fold,  $n = 26$ ; POAG:  $2.52 \pm 0.55$  fold,  $n = 26$ ;  $P = 0.011$ ). However, hsa-miR-885-5p was not significantly differentially expressed in the serum of POAG patients and controls in the screening set (Hsa-miR-885-5p:

TABLE 2. Differentially Expressed miRNAs Among the POAG and Control Groups

No.	miRNA ID	Log2 Ratio, POAG/Control	Probability
1	hsa-miR-885-5p	11.30501671	0.816935918
2	hsa-miR-210-3p	8.347469391	0.803177167
3	hsa-miR-3149	10.74763356	0.801669359

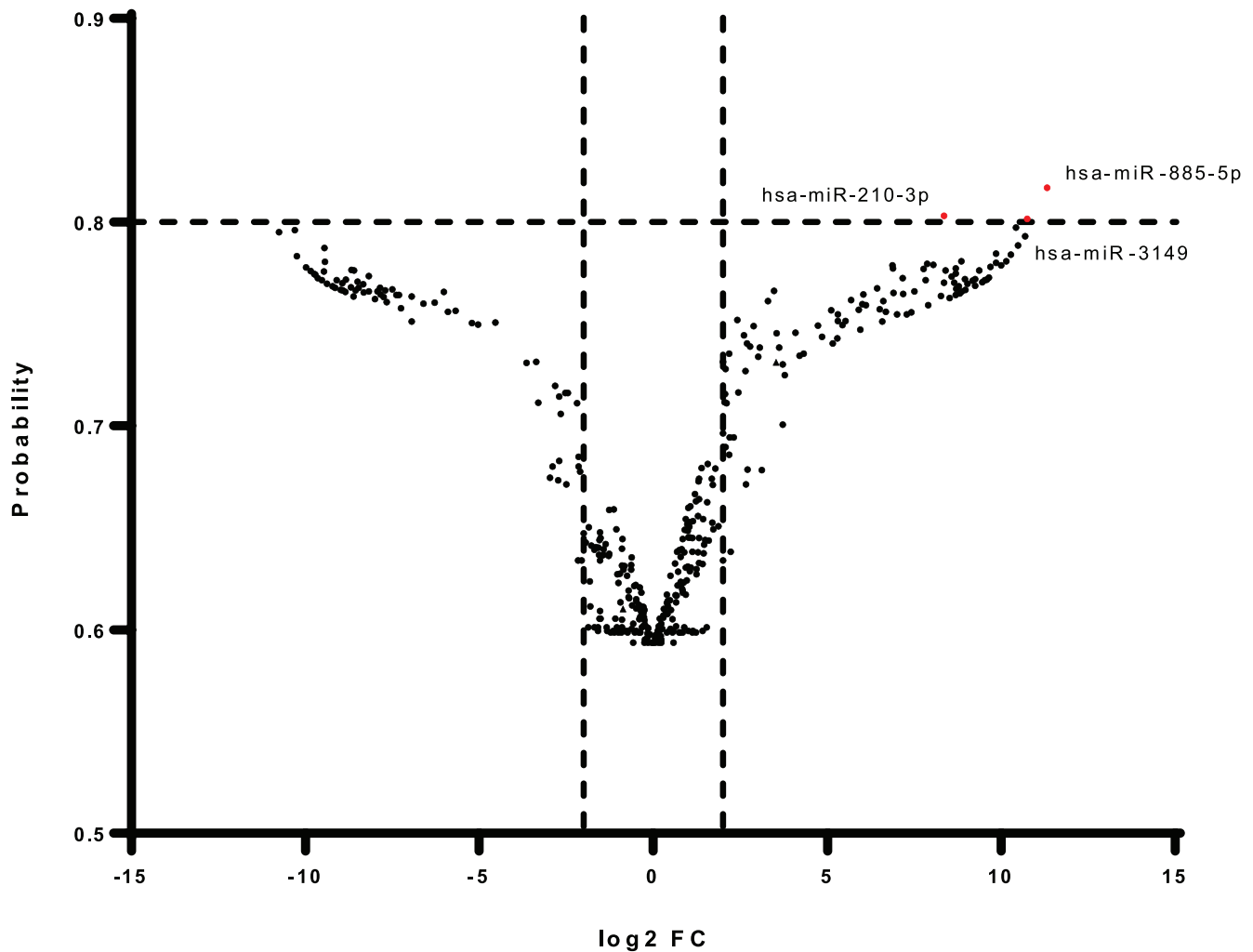


FIGURE 2. Volcano plot showing differentially expressed miRNAs. Three miRNAs were identified as differentially expressed, with a fold change greater than 4 and probability score greater than 0.8, between POAG patients and matched controls. Red dots represent significantly upregulated miRNAs in POAG eyes.

control:  $1.22 \pm 0.18$  fold,  $n = 26$ ; POAG:  $1.44 \pm 0.32$  fold,  $n = 26$ ;  $P = 0.551$ ) and was excluded from further analysis in the validation set.

To further validate these results, we examined the circulating levels of hsa-miR-210-3p in an independent sample of 33 POAG patients and 33 controls (Fig. 4). Again, hsa-miR-210-3p showed significantly elevated expression levels in the POAG patients, compared to the controls (Hsa-miR-210-3p: control:  $1.22 \pm 0.15$  fold,  $n = 33$ ; POAG:  $2.54 \pm 0.39$  fold,  $n = 33$ ;  $P = 0.002$ ).

**ROC Analysis of miRNAs Diagnosing POAG and Different Stages of POAG**

The role of hsa-miR-210-3p in diagnosing POAG was further demonstrated by constructing the ROC curve. In the screening set, the area under the curve (AUC) was 0.846, corresponding to a specificity of 84.6% and sensitivity of 80.8% for hsa-miR-210-3p, and 0.527, corresponding to a specificity of 53.8% and sensitivity of 57.7% for hsa-miR-885-5p. In the validation set, the AUC of hsa-miR-210-3p for distinguishing POAG was 0.813 (sensitivity: 84.8%; specificity: 69.7%; Fig. 5).

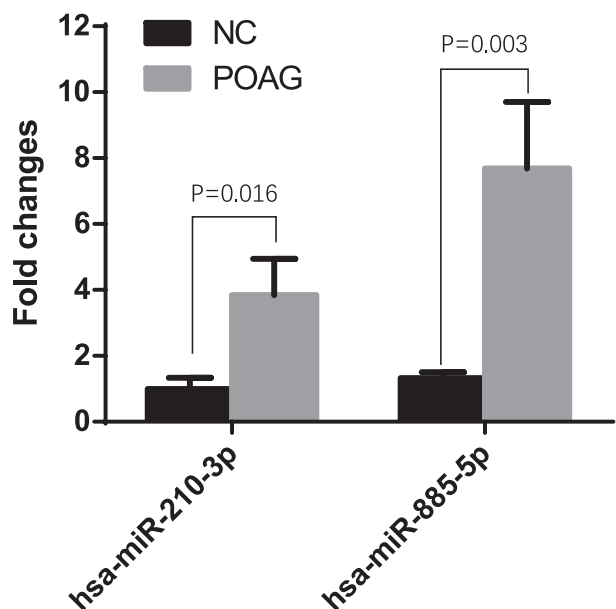


FIGURE 3. Confirmation of miRNA level (mean with SEM) of sequenced serum samples by qRT-PCR.

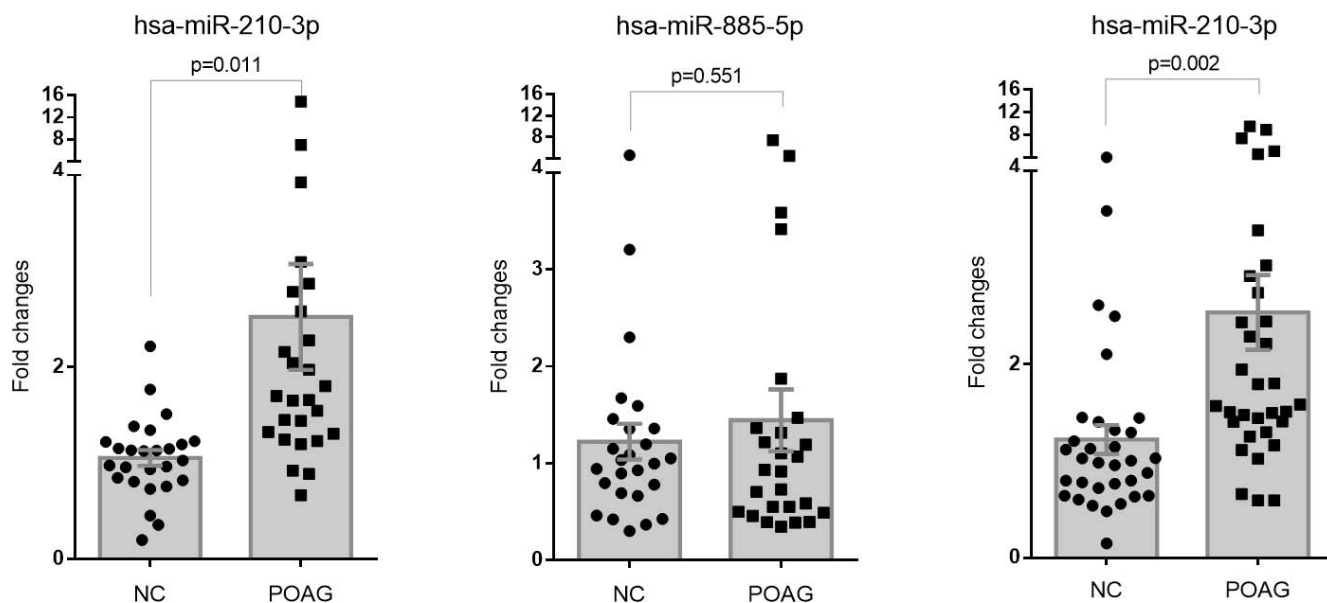


FIGURE 4. miRNA levels of hsa-miR-210-3p (in the screening set and the validation set) and hsa-miR-885-5p (in the screening set) by qRT-PCR. Bars: mean with SEM.

We also examined the capacity of miRNA expression to distinguish between severe and mild glaucoma using ROC analysis. The patient was defined as a mild POAG patient when the MD  $\geq -6$  dB in both eyes, and as a severe POAG patient when the MD  $< -6$  dB in at least one eye. On pooling all participants from the screening and validation sets (Fig. 6), hsa-miR-210-3p differentiated between severe POAG patients and controls with an AUC of 0.880 (sensitivity: 85.4%; specificity: 85.7%), between mild POAG patients and controls with an AUC of 0.692 (sensitivity: 66.7%; specificity: 74.3%), and between severe and mild POAG patients with an AUC of 0.738 (sensitivity: 63.4%; specificity: 66.7%). Linear regressions were used to characterize the relationship of the hsa-miR-210-3p expression levels with the patients' IOP, MD, and RNFLT $\alpha$  of the more severe eye, the milder eye, and the average of both eyes, separately. The expression level of hsa-miR-210-3p was significantly correlated with the MD and RNFLT $\alpha$  of the patients' more severe eye (Table 3, Fig. 7). Hsa-miR-210-3p was also significantly associated with the patients' binocular

average MD without adjustment (Supplementary Table S1). No associations were found between hsa-miR-210-3p and IOP, MD, or RNFLT $\alpha$  of the patients' milder eye (see Supplementary Table S2).

### DISCUSSION

In the present study, we identified miRNA profiles in serum from POAG patients and matched control subjects using next-generation sequencing and qRT-PCR in a sequencing phase, screening phase, and validation phase. Hsa-miR-210-3p was found to be elevated in POAG patients in all phases. On performing ROC analysis for the screening and validation sets, hsa-miR-210-3p was found to differentiate between POAG patients and matched controls with an AUC of 0.846 (sensitivity: 84.6%; specificity: 80.8%) and 0.813 (sensitivity: 84.8%; specificity: 69.7%), respectively. In addition, the expression of hsa-miR-210-3p was associated with the MD value of visual field defects and RNFLT $\alpha$  of the POAG patients.

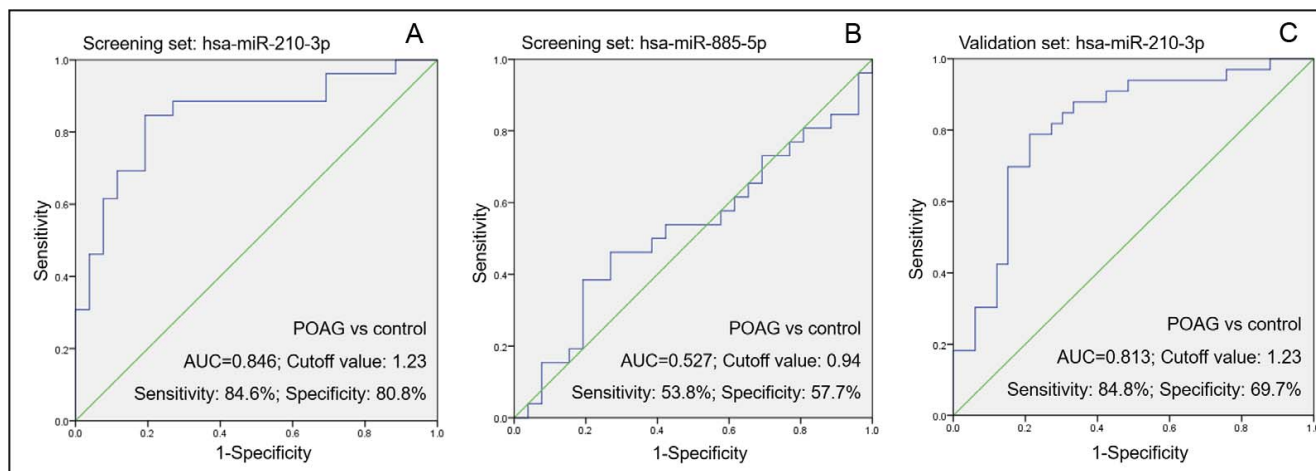


FIGURE 5. ROC analysis of miRNAs in distinguishing POAG patients from controls. (A) hsa-miR-210-3p in the screening set, (B) hsa-miR-885-5p in the screening set, and (C) hsa-miR-210-3p in the validation set.

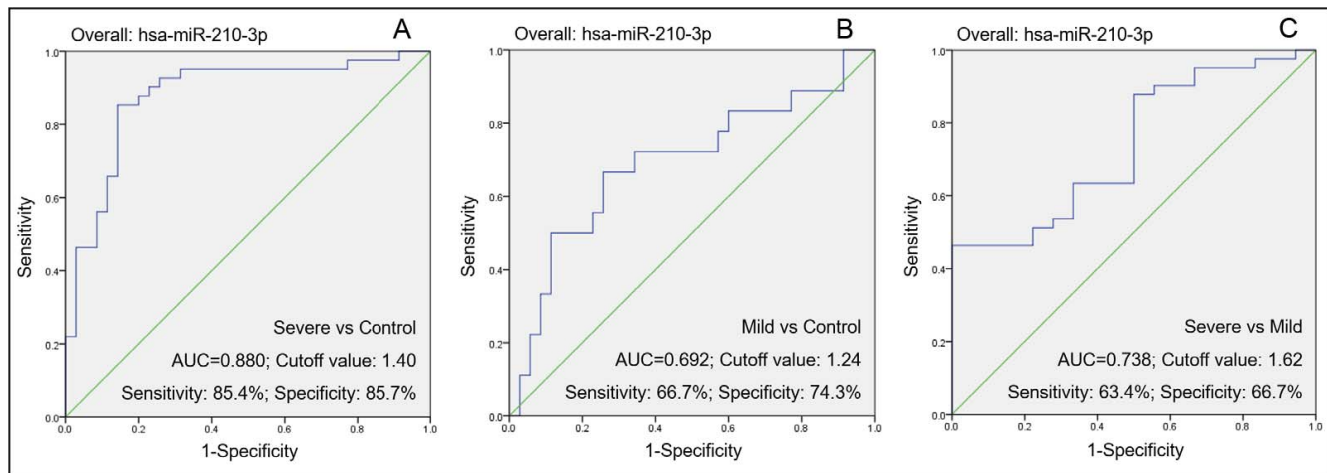


FIGURE 6. ROC analysis of hsa-miR-210-3p in distinguishing different stages of POAG. (A) hsa-miR-210-3p differentiated between severe POAG patients and controls, (B) hsa-miR-210-3p differentiated between mild POAG patients and controls, and (C) hsa-miR-210-3p differentiated between severe and mild POAG patients.

Thus, we consider hsa-miR-210-3p to have a potential clinical utility as a diagnostic marker for POAG.

To our knowledge, the ROC curve obtained for hsa-miR-210-3p in our study is unprecedented for blood-based POAG biomarkers. Previous studies have found various POAG biomarkers from serum, plasma, or leukocytes of the peripheral blood, including oxidation related, vascular related, immune related, and other markers, as summarized and roughly classified in Table 4.<sup>24-45</sup> However, we have found only one study reporting the ROC analysis of a blood-based biomarker, which revealed that the AUC indicating the ability of the neutrophil-to-lymphocyte ratio to distinguish patients with POAG from controls was 0.651, with a sensitivity of 65% and a specificity of 65%.<sup>44</sup> In our study, we found that hsa-miR-210-3p is more effective in differentiating between POAG patients and matched controls, with an AUC of 0.846 (sensitivity: 84.6%; specificity: 80.8%) and 0.813 (sensitivity: 84.8%; specificity: 69.7%) in the screening and validation sets, respectively. The methodology used in our study is also unsurpassed in the POAG biomarker field. The strengths of our study include (1) the use of RNA sequencing in the sequencing phase; (2) screening and validation in two independent samples; and (3) inclusion of patients with

varying degrees of optic neuropathy. In addition, most blood-based biomarkers found in previous studies are proteins, mRNAs, or intermediate metabolites, which are not as stable as miRNAs.

Moreover, hsa-miR-210-3p differentiated between severe POAG patients and controls with an AUC of 0.880 (sensitivity: 85.4%; specificity: 85.7%), between mild POAG patients and controls with an AUC of 0.692 (sensitivity: 66.7%; specificity: 74.3%), and between severe and mild POAG patients with an AUC of 0.738 (sensitivity: 63.4%; specificity: 66.7%). This indicated that circular hsa-miR-210-3p might be better at diagnosing severe POAG patients than mild POAG patients. The expression of hsa-miR-210-3p was associated with the POAG patients' MD and RNFLTα visual field defects of the more severe eye, rather than those of the milder eye. Therefore, we believe that the elevation of hsa-miR-210-3p mainly depends on information obtained from the eye with the more severe visual function defects. Although the capacity of hsa-miR-210-3p expression to distinguish mild and severe glaucoma is still relatively low, we believe that it is a promising biomarker whose capacity to serve as a biomarker will be improved if it is studied using a larger sample size or when coupled with other potential blood-based biomarkers.

The precise cellular sources and mechanisms underlying the observed elevations of hsa-miR-210-3p expression are yet to be determined, but previous studies have provided important clues regarding this aspect. MiR-210-3p was well studied as a micromanager of the hypoxia pathway.<sup>46</sup> Hsa-miR-210-3p may act as a circulating factor in response to hypoxic environments at high altitudes.<sup>47</sup> Microarray analysis has shown that its induction was the most significant under hypoxic conditions. The regulation of hsa-miR-210 by hypoxia was mediated by the hypoxia-inducible factor-1α (HIF-1α)/VHL transcriptional system and/or HIF-2α.<sup>48-50</sup> Consistently, studies have shown that exosomal miR-210-3p could be delivered into endothelial cells and directly inhibit the expression of SMAD4 and STAT6, resulting in enhanced angiogenesis.<sup>51</sup> However, many previous researchers have shown that miR-210 upregulation could cause harm to various kinds of cells. For instance, the expression of hsa-miR-210-3p led to placental mitochondrial dysfunction and oxidative stress.<sup>52</sup> Upregulation of rno-miR-210-3p under acute cold stress conditions was shown to enhance the mitochondrial respiratory capacity of cells, but caused cell death.<sup>53</sup> In addition, the elevation of miR-210-3p expression was shown to contribute to dopamine neuron

TABLE 3. The Relationship Between the hsa-miR-210-3p Expression Level and Patients' IOP, MD, and RNFLTα of the More Severe Eye

Items	B	SE	95% CI	P Value
hsa-miR-210-3p (Lg transformed)				
IOP				
Model 1*	1.024	0.534	(-0.047, 2.095)	0.060
Model 2†	0.763	0.557	(-0.335, 1.881)	0.177
MD  (Ln transformed)				
Model 1	0.298	0.095	(0.107, 0.489)	<b>0.003</b>
Model 2	0.237	0.100	(0.035, 0.438)	<b>0.022</b>
RNFLTα				
Model 1	-6.228	2.156	(-10.556, 1.899)	<b>0.006</b>
Model 2	-5.792	2.257	(-10.338, -1.246)	<b>0.014</b>

P values are bolded when smaller than 0.05. |MD|, the absolute value of mean deviation; Lg, logarithm with base 10.

\* Logistic regression of the presence of glaucoma without adjusting for any covariates.

† Logistic regression of the presence of glaucoma adjusted for age, sex, and glaucoma medication.

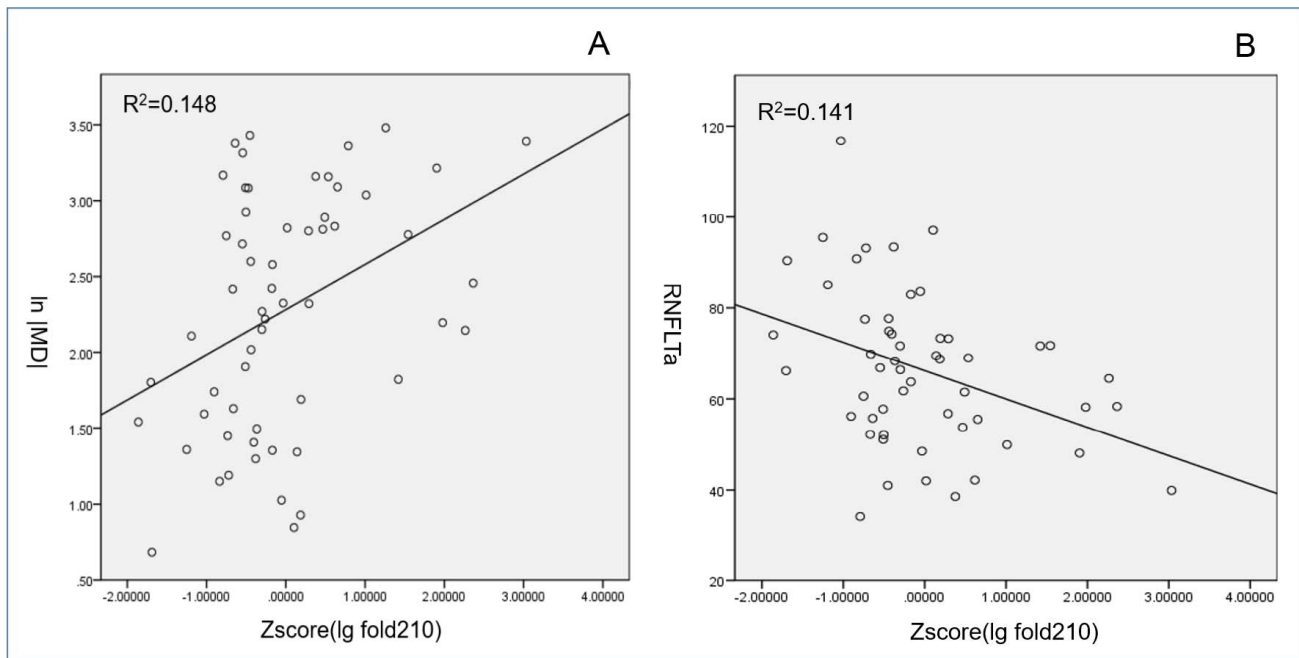


FIGURE 7. Linear regressions characterizing the relationship of hsa-miR-210-3p expression levels with MD (A) and RNFLTα (B) of the more severe eye, adjusted for age, sex, and glaucoma medication. Fold210 is the relative expression of hsa-miR-210-3p. |MD| is the absolute value of MD.

damage by reducing brain-derived neurotrophic factor production.<sup>54</sup> It is generally agreed that the increase in IOP and vascular dysregulation are two important causes of glaucoma; they can cause ischemia and hypoxia in the components of the optic nerve head and thus induce mitochondrial dysfunction and oxidative stress.<sup>55,56</sup> Therefore, we speculate that hypoxia in the retina of an eye with glaucoma may induce the elevation of hsa-miR-210-3p expression, which may enhance mitochon-

drial dysfunction and oxidative stress in retinal ganglion cells (RGCs) and lead to RGC death and RNFL thinning. Previous studies by our group and others,<sup>13,57,58</sup> however, did not find the expression of hsa-miR-210-3p to be changed in the aqueous humor of the eyes of POAG patients, indicating that the elevation of hsa-miR-210-3p levels in blood may not be due to the direct release of hsa-miR-210-3p from the eyes of POAG patients. The expression of miRNAs in the aqueous humor is

TABLE 4. Blood-Based Biomarkers of POAG Reported in Previous Studies

Biomarker Classification	Components Detected	Biomarkers	References
Oxidation related	Plasma	Superoxide dismutase 1	Canizales et al. <sup>24</sup> (2016)
	Plasma	cGMP and NO <sub>2</sub>	Galassi et al. <sup>25</sup> (2004)
	Serum	Malondialdehyde, total antioxidant capacity, ATP/ADP	Nucci et al. <sup>26</sup> (2013)
	Serum	Protein carbonyls and advanced glycation end products	Hondur et al. <sup>27</sup> (2017)
	Plasma	Homocysteine	Roedel et al. <sup>28</sup> (2007)
	Plasma	Vitamin E, vitamin C, glutathione peroxidase	Zanon-Moreno et al. <sup>29</sup> (2013)
	Serum	Lipofuscin, malondialdehyde, mitochondrial isoform of superoxide dismutase, activity of total superoxide dismutase	Rokicki et al. <sup>30</sup> (2017)
Vascular related	Plasma	Endothelin-1, homocysteine	López-Riquelme et al. <sup>31</sup> (2014)
	Plasma	N-terminal fragment of the proatrial natriuretic peptide	Baumane et al. <sup>32</sup> (2017)
	Serum	Erythropoietin, soluble CD44	Mokbal et al. <sup>33</sup> (2010)
	Plasma	Prothrombin fragments 1+2, D-dimer, fibrinogen	O'Brien et al. <sup>34</sup> (1997)
Immune related	Blood	T-cell subsets, soluble interleukin-2 receptor/interleukin-2	Yang et al. <sup>35</sup> (2001)
	Blood	Neutrophil-to-lymphocyte ratio and platelet-to-lymphocyte ratio	Ozgonul et al. <sup>44</sup> (2016)
	Serum	28 IgG V domain peptides	Schmelter et al. <sup>36</sup> (2017)
Other markers	Leukocytes	Transient receptor potential cation channel 6 gene	Chen et al. <sup>37</sup> (2013)
	Serum	Brain-derived neurotrophic factor	Ghaffariyeh et al. <sup>38</sup> (2011)
	Plasma	Testosterone	Kang et al. <sup>39</sup> (2018)
	Serum	3α-Hydroxysteroid dehydrogenase activity	Weinstein et al. <sup>40</sup> (1996)
	Plasma	20S Proteasome α-subunit	Wunderlich et al. <sup>45</sup> (2002)
	Serum	CFH, C3, FBLN1, ALB, ITIH4, TF, APOA1, VTN, APOA4, IGHG2, APCS, APOL1, FCN3, SERPINA1, C4A, SERPINC1, TTR	González-Iglesias et al. <sup>42</sup> (2014)
	Serum	Apoptosis-inducing factor, cyclic AMP-responsive element binding protein, ephrin type-A receptor, huntingtin	Tezel et al. <sup>43</sup> (2012)

not totally representative of, and may partly reflect, that in the retina. There is also a hypothesis that systemic mitochondrial dysfunction itself is an original cause, rather than a consequence, of glaucoma-related neurodegeneration. Using conventional and next-generation massively parallel sequencing, a recent publication has reported that 50% of POAG cases show pathogenic mtDNA mutations. Approximately one-third of mutations were in one of the complex-I mitochondrial genes (*ND5* gene).<sup>59</sup> Complex-I defects have been demonstrated in the lymphoblasts of POAG patients, leading to decreased rates of respiration and ATP production.<sup>60</sup> Taken together with various dysregulated oxidation-related factors found in previous studies, we also assume that the elevation of hsa-miR-210-3p itself may be a signal of systemic mitochondrial dysfunction and thus be a cause of POAG. Overall, based on previously published studies, there may be several ways to explain the elevated miR-210-3p levels in the blood of POAG patients: (1) Hypoxia in the retina of an eye of a patient with glaucoma may induce the elevation of hsa-miR-210-3p expression; however, previous studies by our group and others<sup>13,57,58</sup> have not detected elevated miR-210-3p levels in the aqueous humor of eyes of POAG patients. This implies that the miR-210-3p in the blood may not come directly from the retina. Hypoxia in the retina of eyes of glaucoma patients may release certain signals that are still unknown to us and then induce the increase in hsa-miR-210-3p expression. (2) Previous studies have found that systemic mitochondrial dysfunction was detected in POAG patients<sup>55,56,59,60</sup>; therefore, we assume that the elevation of hsa-miR-210-3p itself may be a signal of systemic mitochondrial dysfunction related to POAG. However, whether the upregulated miR-210-3p in the blood crosses the blood-retinal barrier to act on the retina or mitochondrial dysfunction occurs at the same time in the retina and increases the miR-210-3p expression at local sites remains to be ascertained. Further studies are needed to determine whether the elevation of hsa-miR-210-3p is a cause, a result, and/or a concomitant factor of POAG.

However, our study has a few limitations. First, the quantification of miRNAs by miRNA sequencing and qRT-PCR is influenced by sample preparation, including RNA isolation<sup>61</sup> and cDNA preparation,<sup>62</sup> and is dependent on the platform used.<sup>23</sup> However, by using two different methodologies, we aimed at controlling these potential sources of bias, and hence, identifying true disease-related microRNAs. Second, in our study subjects were recruited from a single center, with a relatively small sample size. A future multicenter longitudinal study with a larger number and heterogeneous groups of patients should be performed to strengthen these results by testing the effects of multiple covariates. Third, the relatively low cutoff value of 1.23 for differentiating between POAG patients and normal subjects limits the clinical usage of this biomarker due to the current technical limitations of qRT-PCR with regard to precision. In future studies, we will verify the elevation of miR-210-3p using absolute quantification rather than relative quantification of miRNA expression; this will make it more widely applicable in clinical practice. In addition, patients with different ocular diseases such as primary angle-closure glaucoma and age-related macular degeneration are also needed to further calculate the biomarker sensitivity/specificity of circulating hsa-miR-210-3p for diagnosing POAG.

In conclusion, circulating hsa-miR-210-3p is associated with POAG with a higher specificity and sensitivity than other previously identified blood-based biomarkers. Thus, circulating hsa-miR-210-3p was identified as a potential diagnostic marker for POAG (especially for severe POAG patients). These results, however, should be interpreted with caution. As stated previously, future studies are needed to test the robustness of hsa-miR-210-3p as a biomarker for POAG.

## Acknowledgments

Supported by the National Natural Science Foundation of China (81670847, 81600728) and the Fundamental Research Funds of the State Key Laboratory of Ophthalmology. The funding organizations had no role in the design or conduct of this research.

Disclosure: **Y. Liu**, None; **Y. Wang**, None; **Y. Chen**, None; **X. Fang**, None; **T. Wen**, None; **M. Xiao**, None; **S. Chen**, None; **X. Zhang**, None

## References

- Jonas JB, Aung T, Bourne RR, Bron AM, Ritch R, Panda-Jonas S. Glaucoma. *Lancet*. 2017;390:2183-2193.
- Tham YC, Li X, Wong TY, Quigley HA, Aung T, Cheng CY. Global prevalence of glaucoma and projections of glaucoma burden through 2040: a systematic review and meta-analysis. *Ophthalmology*. 2014;121:2081-2090.
- Aldridge S, Hadfield J. Introduction to miRNA profiling technologies and cross-platform comparison. *Methods Mol Biol*. 2012;822:19-31.
- Filipowicz W, Bhattacharyya SN, Sonenberg N. Mechanisms of post-transcriptional regulation by microRNAs: are the answers in sight? *Nat Rev Genet*. 2008;9:102-114.
- Wang J, Chen J, Sen S. MicroRNA as biomarkers and diagnostics. *J Cell Physiol*. 2016;231:25-30.
- Hayes J, Peruzzi PP, Lawler S. MicroRNAs in cancer: biomarkers, functions and therapy. *Trends Mol Med*. 2014;20:460-469.
- Wang Y, Gu J, Roth JA, et al. Pathway-based serum microRNA profiling and survival in patients with advanced stage non-small cell lung cancer. *Cancer Res*. 2013;73:4801-4809.
- Kondkar AA, Abu-Amero KK. Utility of circulating microRNAs as clinical biomarkers for cardiovascular diseases [published online ahead of print February 1, 2015]. *Biomed Res Int*. doi:10.1155/2015/821823.
- Fang L, Ellims AH, Moore XL, et al. Circulating microRNAs as biomarkers for diffuse myocardial fibrosis in patients with hypertrophic cardiomyopathy. *J Transl Med*. 2015;13:314.
- McClelland AD, Kantharidis P. MicroRNA in the development of diabetic complications. *Clin Sci*. 2014;126:95-110.
- Delić D, Eisele C, Schmid R, et al. Urinary exosomal miRNA signature in type II diabetic nephropathy patients. *PLoS One*. 2016;11:e0150154.
- Ertekin S, Yildirim O, Dinc E, Ayaz L, Fidanci SB, Tamer L. Evaluation of circulating miRNAs in wet age-related macular degeneration. *Mol Vis*. 2014;20:1057-1066.
- Liu Y, Chen Y, Wang Y, et al. MicroRNA profiling in glaucoma eyes with varying degrees of optic neuropathy by using next-generation sequencing. *Invest Ophthalmol Vis Sci*. 2018;59:2955-2966.
- Wang W, Du S, Zhang X. Corneal deformation response in patients with primary open-angle glaucoma and in healthy subjects analyzed by corvis ST. *Invest Ophthalmol Vis Sci*. 2015;56:5557-5565.
- Cock PJA, Fields CJ, Goto N, Heuer ML, Rice PM. The Sanger FASTQ file format for sequences with quality scores, and the Solexa/Illumina FASTQ variants. *Nucleic Acids Res*. 2010;38:1767-1771.
- Kozomara A, Griffiths-Jones S. MiRBase: annotating high confidence microRNAs using deep sequencing data. *Nucleic Acids Res*. 2014;42:D68-D73.
- Friedländer MR, Chen W, Adamidi C, et al. Discovering microRNAs from deep sequencing data using miRDeep. *Nat Biotechnol*. 2008;26:407-415.
- 't Hoen PAC, Ariyurek Y, Thygesen HH, et al. Deep sequencing-based expression analysis shows major advances

- in robustness, resolution and inter-lab portability over five microarray platforms. *Nucleic Acids Res.* 2008;36:e141.
19. Hughes AE, Bradley DT, Campbell M, et al. Mutation altering the miR-184 seed region causes familial keratoconus with cataract. *Am J Hum Genet.* 2011;89:628-633.
  20. Tarazona S, García-Alcalde F, Dopazo J, Ferrer A, Conesa A. Differential expression in RNA-seq: a matter of depth. *Genome Res.* 2011;21:2213-2223.
  21. Schwarzenbach H, da Silva AM, Calin G, Pantel K. Data normalization strategies for microRNA quantification. *Clin Chem.* 2015;61:1333-1342.
  22. Livak KJ, Schmittgen TD. Analysis of relative gene expression data using real-time quantitative PCR and the 2- $\Delta\Delta$ CT method. *Methods.* 2001;25:402-408.
  23. Mestdagh P, Hartmann N, Baeriswyl L, et al. Evaluation of quantitative miRNA expression platforms in the microrna quality control (mirQC) study. *Nat Methods.* 2014;11:809-815.
  24. Canizales L, Rodriguez L, Rivera C, Martinez A, Mendez F, Castillo A. Low-level expression of SOD1 in peripheral blood samples of patients diagnosed with primary open-angle glaucoma. *Biomark Med.* 2016;10:1219-1223.
  25. Galassi F, Renieri G, Sodi A, Ucci F, Vannozzi L, Masini E. Nitric oxide proxies and ocular perfusion pressure in primary open angle glaucoma. *Br J Ophthalmol.* 2004;88:757-760.
  26. Nucci C, Di Pierro D, Varesi C, et al. Increased malondialdehyde concentration and reduced total antioxidant capacity in aqueous humor and blood samples from patients with glaucoma. *Mol Vis.* 2013;19:1841-1846.
  27. Hondur G, Göktaş E, Yang X, et al. Oxidative stress-related molecular biomarker candidates for glaucoma. *Invest Ophthalmol Vis Sci.* 2017;58:4078-4088.
  28. Roedl JB, Bleich S, Reulbach U, et al. Homocysteine levels in aqueous humor and plasma of patients with primary open-angle glaucoma. *J Neural Transm.* 2007;114:445-450.
  29. Zanon-Moreno V, Asensio-Marquez EM, Ciancotti-Oliver L, et al. Effects of polymorphisms in vitamin E-, vitamin C-, and glutathione peroxidase-related genes on serum biomarkers and associations with glaucoma. *Mol Vis.* 2013;19:231-242.
  30. Rokicki W, Zaleska-Fiolka J, Pojda-Wilczek D, et al. Differences in serum oxidative status between glaucomatous and nonglaucomatous cataract patients. *BMC Ophthalmol.* 2017;17:13.
  31. López-Riquelme N, Villalba C, Tormo C, et al. Endothelin-1 levels and biomarkers of oxidative stress in glaucoma patients. *Int Ophthalmol.* 2014;35:527-532.
  32. Baumane K, Ranka R, Laganovska G. Association of NT-proANP level in plasma and humor aqueous with primary open-angle glaucoma. *Curr Eye Res.* 2017;42:233-236.
  33. Mokbel TH, Ghanem AA, Kishk H, Arafa LF, El-Baiomy AA. Erythropoietin and soluble CD44 levels in patients with primary open-angle glaucoma. *Clin Exp Ophthalmol.* 2010;38:560-565.
  34. O'Brien C, Butt Z, Ludlam C, Detkova P, Drance SM. Activation of the coagulation cascade in untreated primary open-angle glaucoma. *Ophthalmology.* 1997;104:725-730.
  35. Yang J, Patil RV, Yu H, Gordon M, Wax MB. T cell subsets and sIL-2R/IL-2 levels in patients with glaucoma. *Am J Ophthalmol.* 2001;131:421-426.
  36. Schmelter C, Perumal N, Funke S, Bell K, Pfeiffer N, Grus FH. Peptides of the variable IgG domain as potential biomarker candidates in primary open-angle glaucoma (POAG). *Hum Mol Genet.* 2017;26:4451-4464.
  37. Chen S, Fan Q, Gao X, et al. Increased expression of the transient receptor potential cation channel 6 gene in patients with primary open-angle glaucoma. *Clin Exp Ophthalmol.* 2013;41:753-760.
  38. Ghaffariyeh A, Honarpisheh N, Heidari MH, Puyan S, Abasov F. Brain-derived neurotrophic factor as a biomarker in primary open-angle glaucoma. *Optom Vis Sci.* 2011;88:80-85.
  39. Kang JH, Rosner BA, Wiggs JL, Pasquale LR. Sex hormone levels and risk of primary open-angle glaucoma in postmenopausal women. *Menopause.* 2018;25:1116-1123.
  40. Weinstein BI, Iyer RB, Binstock JM, et al. Decreased 3 $\alpha$ -hydroxysteroid dehydrogenase activity in peripheral blood lymphocytes from patients with primary open angle glaucoma. *Exp Eye Res.* 1996;62:39-45.
  41. Wunderlich K, Golubnitschaja O, Pache M, Eberle A-N, Flammer J. Increased plasma levels of 20S proteasome alpha-subunit in glaucoma patients: an observational pilot study. *Mol Vis.* 2002;8:431-435.
  42. González-Iglesias H, Álvarez L, García M, et al. Comparative proteomic study in serum of patients with primary open-angle glaucoma and pseudoexfoliation glaucoma. *J Proteomics.* 2014;98:65-78.
  43. Tezel G, Thornton IL, Tong MG, et al. Immunoproteomic analysis of potential serum biomarker candidates in human glaucoma. *Invest Ophthalmol Vis Sci.* 2012;53:8222-8231.
  44. Ozgonul C, Sertoglu E, Mumcuoglu T, Kucukevcilioglu M. Neutrophil-to-lymphocyte ratio and platelet-to-lymphocyte ratio as novel biomarkers of primary open-angle glaucoma. *J Glaucoma.* 2016;25:e815-e820.
  45. Wunderlich K, Golubnitschaja O, Pache M, Eberle A-N, Flammer J. Increased plasma levels of 20S proteasome alpha-subunit in glaucoma patients: an observational pilot study. *Mol Vis.* 2002;8:431-435.
  46. Huang X, Le QT, Giaccia AJ. MiR-210—micromanager of the hypoxia pathway. *Trends Mol Med.* 2010;16:230-237.
  47. Yan Y, Wang C, Zhou W, et al. Elevation of circulating miR-210-3p in high-altitude hypoxic environment. *Front Physiol.* 2016;7:84.
  48. McCormick RI, Blick C, Ragoussis J, et al. MiR-210 is a target of hypoxia-inducible factors 1 and 2 in renal cancer, regulates ISCU and correlates with good prognosis. *Br J Cancer.* 2013;108:1133-1142.
  49. Camps C, Buffa FM, Colella S, et al. Hsa-miR-210 is induced by hypoxia and is an independent prognostic factor in breast cancer. *Clin Cancer Res.* 2008;14:1340-1348.
  50. Kulshreshtha R, Ferracin M, Wojcik SE, et al. A MicroRNA signature of hypoxia. *Mol Cell Biol.* 2007;27:1859-1867.
  51. Lin XJ, Fang JH, Yang XJ, et al. Hepatocellular carcinoma cell-secreted exosomal microRNA-210 promotes angiogenesis in vitro and in vivo. *Mol Ther Nucleic Acids.* 2018;11:243-252.
  52. Muralimanoharan S, Maloyan A, Mele J, Guo C, Myatt LG, Myatt L. MIR-210 modulates mitochondrial respiration in placenta with preeclampsia. *Placenta.* 2012;33:816-823.
  53. Guo W, Lian S, Zhen L, et al. Cellular physiology and biochemistry cellular physiology and biochemistry the favored mechanism for coping with acute cold stress: upregulation of miR-210 in rats. *Cell Physiol Biochem.* 2018;46:2090-2102.
  54. Liu X, Kiss GK, Mellender SJ, Weiss HR, Chi OZ. Activation of Akt by SC79 decreased cerebral infarct in early cerebral ischemia-reperfusion despite increased BBB disruption. *Neurosci Lett.* 2018;681:78-82.
  55. Kamel K, Farrell M, O'Brien C. Mitochondrial dysfunction in ocular disease: focus on glaucoma. *Mitochondrion.* 2017;35:44-53.
  56. Osborne NN, Núñez-Álvarez C, Joglar B, del Olmo-Aguado S. Glaucoma: focus on mitochondria in relation to pathogenesis and neuroprotection. *Eur J Pharmacol.* 2016;787:127-133.
  57. Jayaram H, Phillips JI, Lozano DC, et al. Comparison of microRNA expression in aqueous humor of normal and

- primary open-angle glaucoma patients using PCR arrays: a pilot study. *Invest Ophthalmol Vis Sci.* 2017;58:2884-2890.
58. Tanaka Y, Tsuda S, Kunikata H, et al. Profiles of extracellular miRNAs in the aqueous humor of glaucoma patients assessed with a microarray system. *Sci Rep.* 2014;4:5089.
  59. Sundaresan P, Simpson DA, Sambare C, et al. Whole-mitochondrial genome sequencing in primary open-angle glaucoma using massively parallel sequencing identifies novel and known pathogenic variants. *Genet Med.* 2015;17:279-284.
  60. Lee S, Sheck L, Crowston JG, et al. Impaired complex-I-linked respiration and ATP synthesis in primary open-angle glaucoma patient lymphoblasts. *Invest Ophthalmol Vis Sci.* 2012;53:2431-2437.
  61. McAlexander MA, Phillips MJ, Witwer KW. Comparison of methods for miRNA extraction from plasma and quantitative recovery of RNA from cerebrospinal fluid. *Front Genet.* 2013;4:3.
  62. Hafner M, Renwick N, Brown M, et al. RNA-ligase-dependent biases in miRNA representation in deep-sequenced small RNA cDNA libraries. *RNA.* 2011;17:1697-1712.